Opt Quant Electron (2016) 48:247
DOI 10.1007/s11082-016-0508-z

Performance analysis of thermally bonded Er^{3+}, Yb^{3+}:glass/Co^{2+}:$MgAl_2O_4$ microchip lasers

J. Mlynczak[1] · N. Belghachem[1] · K. Kopczynski[1] · J. Kisielewski[2] · R. Stepien[2] · M. Wychowaniec[3] · J. Galas[3] · D. Litwin[3] · A. Czyzewski[3]

Received: 9 November 2015 / Accepted: 9 March 2016 / Published online: 23 March 2016

Abstract The new glass as well as Co^{2+}:$MgAl_2O_4$ saturable absorber synthesis, especially developed for thermal bonding, was described. The procedure of thermal bonding was presented. Generation parameters of continuous wave operation at 1.5 μm wavelength were shown. The threshold below 180 mW and slop efficiency over 10 % was reached. Pulse generation in thermally bonded and unbonded as well as monolithic Er^{3+}, Yb^{3+}:glass/Co^{2+}:$MgAl_2O_4$ microchip lasers was compered. The peak power above 10 kW with pulse energy above 32 μJ and pulse width 3.2 ns was achieved.

Keywords Thermal bonding · Microchip laser · Erbium laser · MALO saturable absorber

1 Introduction

Radiation at 1.5 μm wavelength because of its unique properties such as safety for eyes, high transmission in the atmosphere and optical fibres, absorption by body tissue, has found many applications. One of the most interesting one is tele-detection where this radiation is applied to laser range-finders and lidars (Zayhowski and Wilson 2007; Mlynczak et al. 2013). The most desirable laser parameters in such devices are high peak

This article is part of the Topical Collection on Laser Technologies and Laser Applications.

Guest Edited by José Figueiredo, José Rodrigues, Nikolai A. Sobolev, Paulo André and Rui Guerra.

✉ J. Mlynczak
jaroslaw.mlynczak@wat.edu.pl

[1] Institute of Optoelectronics, Military University of Technology, Kaliskiego 2, 00-908 Warsaw, Poland

[2] Institute of Electronic Materials Technology, Wólczyńska 133, 01-919 Warsaw, Poland

[3] Maksymilian Pluta Institute of Applied Optics, Kamionkowska 18, 03-805 Warsaw, Poland

power, high quality of the output beam and simple construction that can be relatively easy achievable by microchip lasers. That is why in the last two decades many papers were published demonstrating operation of such lasers (Laporta et al. 1991; Sourian et al. 1994; Mlynczak et al. 2011; Li et al. 1994; Schweizer et al. 1995; Denker et al. 2002; Mlynczak et al. 2012; Sulc et al. 2009, Chen et al. 2012, 2014a, b; Burov and Krylova 2012; Kisel et al. 2012). The most effective type of the active media used in the microchip lasers operating at 1.5 μm is glass doped with Er^{3+} and Yb^{3+} ions while $MgAl_2O_4$ crystal doped with Co^{2+} ions (MALO) has proved to be the best saturable absorber (Denker et al. 2002; Mlynczak et al. 2012; Karlsson et al. 2000). Very promising technology to improve the peak power, quality of the output beam as well as simplify the construction of such lasers is thermal bonding of the active medium with the saturable absorber (Mlynczak and Belghachem 2015a, b; Belghachem and Mlynczak 2015).

In this paper the synthesis of the glass and MALO, especially developed for thermal bonding applications, as well as the procedure of thermal bonding are presented. Moreover generation parameters of thermally bonded Er^{3+}, Yb^{3+}:glass/Co^{2+}:$MgAl_2O_4$ microchip lasers were analyzed.

2 Laser glass synthesis

The synthesis of phosphate glass was performed using the basic five component system P_2O_5–Al_2O_3–B_2O_3–Yb_2O_3–Li_2O enriched by addition of Er_2O_3 as the active agent. The glass has chemical composition similar to that reported by Karlsson et al. 2002 (Table 1).

This glass can be classified as pyrophosphate glass, because coefficient $R > 1$. According to Ebendorff-Heidepriem et al. 1993 $R = \{[MO] + [M_2O] + 3[M_2O_3]\}/[P_2O_5]$, where concentrations of glass components are expressed in mol%. Glasses with $R = 1$ and $R < 1$ are classified as metaphosphate and ultraphosphate glasses, respectively.

The glass was prepared following the conventional quenching technique using high purity chemicals: P_2O_5 (pure p.a. 99^+ %) and Al_2O_3 (extra pure 99.99 %) from Acros Organics as well as AlF_3 (99.99 % purity), B_2O_3 (99.98 % purity), Yb_2O_3 (REacton 99.99 % purity), Li_2CO_3 (Puratronic 99.998 % purity) and Er_2O_3 (99.99 % purity) from Alfa Aesar. All chemicals were in a powder form. A part of Al_2O_3, equal to 3 wt%, in the prepared batch was replaced by an adequate amount of AlF_3 so as to purify the glass and decrease the amount of OH. During the melting process AlF_3 oxidizes into Al_2O_3 so in the final glass there is no AlF_3.

Appropriate amounts of these chemicals were mixed in a porcelain mortar inside a glove box under dried nitrogen atmosphere. The volatilities of P_2O_5, B_2O_3 and Li_2O, appearing during melting process, in amounts of 20, 15 and 8 % respectively, were taken into account during the preparation of the batch. Carefully mixed powders (for 1000 g portion of glass) were melted in a 1 dm^3 platinum crucible, in an electrical furnace in the

Table 1 Chemical composition of the developed Er^{3+}, Yb^{3+}:phosphate glass

Oxide	P_2O_5	Al_2O_3	B_2O_3	Yb_2O_3	Li_2O	Er_2O_3
mol%	64.20	7.78	11.84	6.91	8.90	0.37
wt%	66.17	5.12	5.99	19.77	1.93	1.02

air atmosphere. After the batch was put into the furnace at 1100–1250 °C, the temperature was increased up to 1350 °C at the rate of 6 °C/min. The glass melt was mixed three times using silica glass rod with 10 mm diameter. The glass melt at 1350 and then at 1380 °C was intensively bubbled during 2 h by ultra-clean and dry oxygen (<0.5 ppm of water content). The oxygen bubbling was applied for better, faster and more effective, homogenization and clarification of the glass melt and for decrease of OH^- ions in the glass structure. Total time of melting and clarifying processes performed at 1350–1380 °C was no less than 5 h. The temperature of the furnace was then decreased to 1250 °C at the rate of 3 °C/min. The glass melt at 1250 °C was cast into a stainless steel mould preheated to 350 °C. The glass block with dimensions of 130 × 115 × 20 mm^3 was then put into electric muffle furnace for careful annealing. After holding it for 1 h at a temperature of 575 °C (10 °C higher than glass transition temperature T_g) it was cooled down (annealed) slowly to the room temperature at the rate of 0.4 °C/min. Using an optical microscope, immediately after casting the glass melt into the mould, it was confirmed that the glass was well melted and without solid, gas or crystalline impurities. Its homogeneity was inspected using polariscopic method and for further technological process only pieces with highest homogeneity were chosen.

The synthesized glass, with its density d = 2.87 g/cm^3, had the Yb^{3+} concentration of 17.3 × 10^{20} ions/cm^3 and the Er^{3+} concentration on the level of 0.89 × 10^{20} ions/cm^3.

3 Growth of $MgAl_2O_4$ single crystals

The single crystals of $MgAl_2O_4$ (MALO) were grown by the Czochralski method using the Oxypuller 20-04 equipment made by Cyberstar (France) with a 40 kW Hüttinger inductive generator. An iridium crucible with 50 mm inner diameter, 52 mm height and 2 mm wall thickness was used. Due to very high melting point of MALO (around 2140 °C) much attention was given to very careful preparation of thermal system. First of all active iridium afterheater with 50 mm inner diameter and 80 mm height placed on crucible edge was used. The crucible was surrounded by single-crystalline zirconia grog and zirconia ceramics. Around afterheater and at the top three layers of zirconia ceramics heat shields were applied.

The batch materials were prepared using MgO (99.995 % purity) and Co_3O_4 (99.99 % purity) from Auer-Remy Lehmann & Voss & Co. as well as Al_2O_3 (99.999 % purity) from MTI Corp. During doping the cobalt was introduced into the batch according to the formula:

$$Mg_{1-x}Co_xAl_2O_4.$$

The growth conditions were as follows:

- atmosphere: pure nitrogen,
- growth direction [111],
- growth rate: 1–2 mm/h,
- rotation rate: 10–30 rpm,
- cooling the single crystal after the growth process: minimum 24 h.

The obtained single crystals up to 75 mm long with 22 mm diameter and intensive blue color were free of inclusions and other macroscopic defects. Some of the crystal rods are presented in Fig. 1.

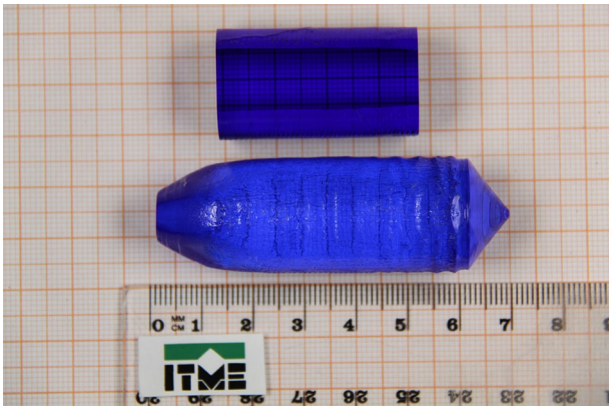

Fig. 1 Two single crystals of MALO

The amount of cobalt in the melt was around 0.085 at.%. The actual content of cobalt in the single crystals was determined using inductively coupled plasma–optical emission spectroscopy (ICP–OES) method. According to the results effective distribution coefficient (describing the ratio of the amount of cobalt incorporated into the MALO crystal to the amount of cobalt put into the crucible) was calculated to be equal to 0.26.

4 Thermal bonding of glass and MALO

4.1 Sample treatment for thermal bonding

The glass and MALO samples were specially prepared for bonding process in the same conditions so as to obtain identical surface quality. The samples of the same hardness were processed together on the same base glass. The dimensions of the prepared glass and MALO samples were equal to 4 × 4 × 1.9 mm and 4 × 4 × 1.4 mm, respectively. Two opposite surfaces (4 × 4 mm) of each sample were polished to obtain the surface parallelism not less than 2 arc sec measured using precision auto collimating lunette and the surface flatness on the level of λ/5 tested by the interferometric method. Samples were bonded to the base glass during the measurement procedure. The quality of the surfaces was of the II cleanness class.

The samples (without the base glass) were tested in the Mach–Zehnder interferometer to obtain the information about the uniformity of the sample's phase and sample quality. The examples of the interferograms of the samples registered in the fringe field as well as in the uniform field modes are presented in Fig. 2 (without phase defects) and in Fig. 3 (with phase defects).

The phase defects were generated during the sample preparation process and reflect non-uniformity of the sample composition. All samples selected for thermal bonding had the optical phase uniformity on the level of λ/4 which was enough to obtain the laser generation.

4.2 Thermal bonding process

The glass and MALO samples were joined together and thermally processed in the melting furnace. Because the furnace was not hermetically sealed the atmosphere inside it was

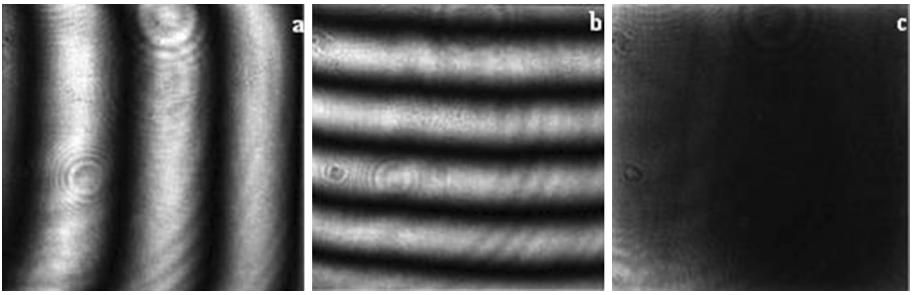

Fig. 2 Interferograms of the sample. Interferograms registered in the fringe field mode (**a**, **b**) and the uniform field mode (**c**)

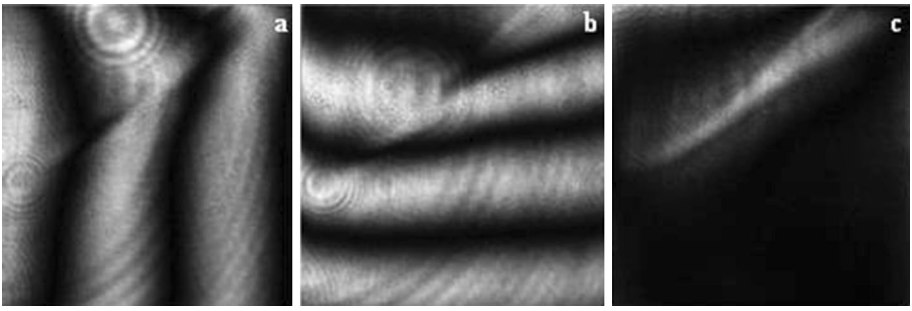

Fig. 3 Interferograms of the sample with the phase defect. Interferograms registered in the fringe field mode (**a**, **b**) and the uniform field mode (**c**)

identical to the ambient (room) atmosphere. Moreover during the process no impact of the air on the bonding between the glass and the crystal was noticed so the atmospheric composition inside the furnace was not controlled. The glass and MALO were bonded under the pressure within the range of 0.2–1 N/mm^2 in the temperature close but not equal to the softening point of glass.

The melting furnace was controlled by the computer software and could generate the desired temperature function of time $\mathbf{T = T(t)}$ as presented in Fig. 4. The temperature function has two ramps: for heating (during the time $\mathbf{t_1}$) and cooling (during the time $\mathbf{t_3}$) processes. The annealing process was performed in constant temperature $\mathbf{T_{max}}$ during the time $\mathbf{t_2}$. The parameters of bonding process were chosen experimentally.

The samples were annealed at the temperature $\mathbf{T_{max}}$ within the range of 500–680 °C. Times $\mathbf{t_1}$, $\mathbf{t_2}$ and $\mathbf{t_3}$ were within the range of 2 h-30 h. The pressure was applied only during the heating and annealing process. The cooling process was not linear. When the temperature reached the $\mathbf{T_{C1}}$, $\mathbf{T_{C2}}$ and $\mathbf{T_{C3}}$ the slope of cooling line was changed. The parameters of the cooling process (i.e.: $\mathbf{T_{Ci}}$ points and the temperature decreasing speed) were chosen experimentally to obtain the best bonding results and to minimize the cooling time. Such approach resulted in reducing internal stresses and bonding the samples more effectively. The whole process gave the good quality optical joint between the glass and the MALO which was also resistive to mechanical and thermal effects.

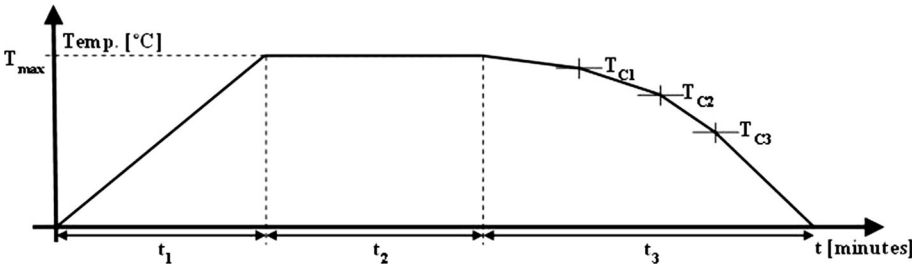

Fig. 4 Bonding process

4.3 Sample processing after thermal bonding

After thermal bonding process the surfaces of the samples were polished again to obtain the parallelism. The MALO crystal was polished to the thickness of 0.29 mm so as to have the small signal transmission for laser radiation equal to 97.5 % (Mlynczak and Belghachem 2015a). The flatness of each surface was tested by interferometric methods and was better than λ/5. The parallelism of the sample's surface was better than 2 arc min (measured using auto-collimation lunette when samples were bonded to the base glass). The residual stresses generated during the polishing process deformed slightly the samples what is visible in the interferograms. Figure 5 presents the example interferograms of four samples after bonding and polishing process registered in the uniform field mode of interferometer. The final phase of the samples (the glass bonded to the spinel) can be described by spheroidal function. The phase front deformation was not greater than 4λ.

The interferometer test allows to visualize the bonding defects which were rather rare. In the defect area the glass and MALO are not bonded. The most probable cause of such type of defects are the local stresses introduced by the cooling process. Typical examples of defects are visible in the Fig. 5c, d (marked by rectangle). For laser experiments only the areas of the samples without the defects were used.

5 Investigation of laser generation

Four glass samples flat and parallel round plates of diameter equal to 8and 1.90 mm long, cut from the same glass block, were examined. First of all, to check the generation capability of the glass cw laser generation was investigated which was already presented in

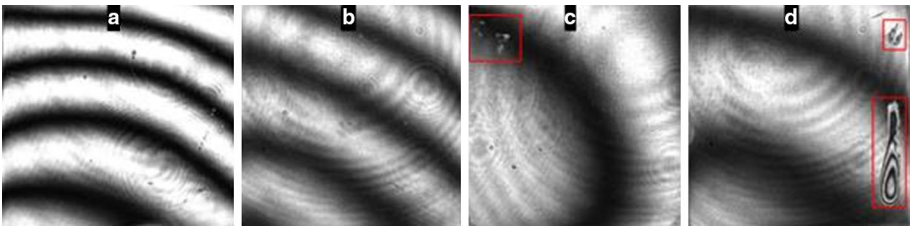

Fig. 5 Example interferograms of the samples after bonding and polishing processes without defects (**a**, **b**) and with defects (**c**, **d**)

paper (Mlynczak and Belghachem 2015c). For this experiment dichroic coatings: antireflection coatings AR at 975 nm and high reflection coatings HR at 1535 nm were deposited on one side of the samples while AR at 1535 nm on the other side. Four output plain-parallel couplers with different reflections R (98.70, 98.15, 97.64, and 96.49 %) at 1535 nm were used. The length of the resonator was equal to the length of the samples. The fiber coupled laser diode with fiber core diameter 100 μm was applied to pump the samples. It operated at 975 nm wavelength in quasi cw regime with period equal to 20 ms and duty-cycle of 50 %. The slope efficiency η and threshold P_{th} are presented in Table 2. The symbol *ng* means that the generation was not achieved. The best parameters were achieved for the first sample characterized by the lowest threshold and quite high slop efficiency. The differences between samples may be caused by some inhomogeneities inside the samples or coatings.

In the second experiment, described in more details in paper (Belghachem and Mlynczak 2015), the same glass samples were used as in the previous experiment. The saturable absorber MALO with small signal transmission equal to 97.5 % and the length equal to 0.29 mm was put inside the resonator and pulse generation was examined. Both sides of MALO had antireflection coatings AR at 1535 nm. The length of the resonator was equal to the sum of the lengths of the active medium and the saturable absorber and it was 2.19 mm. The generation was only achieved for the first sample and only for the output coupler with the highest reflection. This sample was also characterized by the best generation parameters (lowest threshold and quite high slop efficiency) in case of cw generation. The lack of generation for other cases may be caused by too high losses. The generation parameters such as slope efficiency η, threshold P_{th}, peak power P_p, pulse width τ_p, pulse energy E_p, and pulse repetition rate f_r at the pump power 375 mW are presented in Table 3.

In the next experiment the thermally bonded samples were used. This experiment was also described in more details in paper (Belghachem and Mlynczak 2015). The saturable absorbers used in this case had the same small signal transmission equal to 97.5 % and the same length 0.29 mm. The glass samples were not the same but cut from the same glass block as the samples used in the previous two experiments. Both sides of thermally bonded samples were polished. A dichroic plane-parallel input mirror with antireflection coatings at 976 nm on both sides (AR@976 nm) and high reflection coatings at 1535 nm (HR@1535 nm) on one side was used. The length of the cavity and the output couplers were the same as in the previous experiments. The generation parameters are presented in Table 4. The best results were achieved for the second sample where the peak power

Table 2 Slop efficiency η and threshold P_{th} of the investigated samples for different output couplers

Sample	R (%)							
	η (%)				P_{th} (mW)			
	98.70	98.15	97.64	96.49	98.70	98.15	97.64	96.49
1	7.16	7.72	10.35	11.1	178.9	185.0	189.7	205.9
2	9.88	10.16	8.42	8.79	212.2	220.3	246.5	286.1
3	8.22	9.89	8.31	10.58	278.6	286.1	307.1	352.5
4	7.94	8.08	11.42	***ng***	282.9	308.8	331.5	***ng***

Table 3 Generation parameters of unbounded samples

	R (%)	P_p (kW)	τ_p (ns)	E_p (μJ)	η (%)	P_{th} (mW)	f_r (kHz)
Sample 1	98.70	0.35	19.6	6.86	4.52	353	2.220
	98.15	No laser generation					
	97.64	No laser generation					
	96.49	No laser generation					

7.67 kW and pulse length 2.92 ns were reached. The difference of the generation parameters between the investigated samples may be caused by small difference of the length of the saturable absorbers resulting in different small signal transmission or by some inhomogeneities in the glass, the saturable absorber or the joints between them.

During the last experiment, described in more details in paper (Mlynczak and Belghachem 2015b), the input and output mirrors were directly deposited on the thermally bonded samples used in the previous experiment, making monolithic microchip lasers. The characteristic of the input mirror was the same as in case of the previous experiment (high transmission at 975 nm and high reflection at 1535 nm). The output mirror was characterized by partial transmission ($T = 3.5$ %) at 1535 nm. The length of the resonator was also equal to 2.19 mm. The generation parameters are presented in Table 5. The best parameters were again achieved for the second sample where peak power 10.18 kW and pulse length 3.2 ns were reached. The monolithic microchip lasers show similar differences of generation parameters as in the case of thermally bonded samples with external mirrors which can be caused by the same reasons.

Table 4 Generation parameters of thermally bonded samples

	R (%)	P_p (kW)	τ_p (ns)	E_p (μJ)	η (%)	P_{th} (mW)	f_r (kHz)
Sample 1	98.70	3.47	3.36	11.65	3.49	322	1.190
	98.15	2.75	3.40	9.35	3.91	304	1.204
	97.64	6.76	3.24	21.90	14.81	309	1.408
	96.49	4.35	3.44	14.96	3.90	299	0.909
Sample 2	98.70	4.31	2.92	12.49	5.07	285	1.219
	98.15	2.57	4.20	10.79	3.21	284	1.176
	97.64	7.67	2.92	22.39	8.16	309	0.980
	96.49	7.61	3.16	24.04	7.92	301	0.862
Sample 3	98.70	4.61	3.80	17.53	6.06	163	2.553
	98.15	2.49	3.24	8.06	4.47	157	2.342
	97.64	1.83	3.28	6.00	3.12	265	1.693
	96.49	3.76	3.20	12.03	5.80	255	1.785
Sample 4	98.70	2.38	3.44	8.18	4.49	268	2.083
	98.15	1.91	3.40	6.49	2.67	294	1.351
	97.64	2.59	3.04	7.87	3.77	272	1.218
	96.49	3.43	3.64	12.49	6.19	224	1.818

Table 5 Generation parameters of monolithic microchip lasers

Microchip	P_p (kW)	τ_p (ns)	E_p (μJ)	η (%)	P_{th} (mW)	f_r (kHz)
1	7.91	3.6	28.48	5.00	228	0.909
2	10.18	3.2	32.58	5.95	229	0.833
3	5.31	4.0	21.24	3.29	231	0.862
4	6.00	3.9	23.40	5.21	228	0.961

6 Summary

The glass developed especially for thermal bonding can be successfully used for cw generation at 1.5 μm wavelength. The threshold is below 180 mW and slop efficiency over 10 %.

For pulse generation the insertion of MALO saturable absorber inside the resonator is not effective because of the losses which suppress laser operation. A good solution to eliminate the losses is thermal bonding of the active medium with MALO saturable absorber. In such situation using external mirrors the peak power over 7 kW with pulse width below 3 ns can be achieved. However the best generation results are for monolithic microchip lasers where appropriate input and output mirrors are deposited directly on thermally bonded sample Er^{3+}, Yb^{3+}:glass/Co^{2+}:$MgAl_2O_4$. In that case the peak power over 10 kW can be reached.

Acknowledgments The work was sponsored by the Polish National Centre for Research and Development, Project PBS1/B5/16/2012 and Project DOB-1-6/1/PS/2014.

References

Belghachem, N., Mlynczak, J.: Comparison of laser generation in thermally bonded and unbonded $Er3^{+}$, Yb^{3+}:glass/Co^{2+}: $MgAl_2O_4$ microchip lasers. Opt. Mater. **46**, 561–564 (2015)

Burov, L.I., Krylova, L.G.: Optimization of Yb–Er microchip laser parameters. J. Appl. Spectrosc. **79**, 376–381 (2012)

Chen, Y.J., Lin, Y.F., Huang, J.H., Gong, X.H., Luo, Z.D., Huang, Y.D.: Diode-pumped monolithic Er^{3+}:Yb^{3+}:$YAl_3(BO_3)_4$ micro-laser at 1.6 μm. Opt. Commun. **285**, 751–754 (2012)

Chen, Y., Huang, J., Zou, Y., Lin, Y., Gong, X., Luo, Z., Huang, Y.: Diode-pumped passively Q-switched Er^{3+}:Yb^{3+}:$Sr_3Lu_2(BO_3)_4$ laser at 1534 nm. Opt. Exp. **22**, 8333–8338 (2014a)

Chen, Y., Lin, Y., Zou, Y., Huang, J., Gong, X., Luo, Z., Huang, Y.: Diode-pumped 1.5–1.6 μm laser operation in Er^{3+} doped $YbAl_3(BO_3)_4$ microchip. Opt. Exp. **22**, 13969–13974 (2014b)

Denker, B., Galagan, B., Osiko, V., Sverchkov, S.: Materials and components for miniature diode-pumped 1.5 μm erbiglass lasers. Laser Phys. **12**, 697–701 (2002)

Ebendorff-Heidepriem, H., Seeber, W., Ehrt, D.: Dehydration of phosphate glasses. J. Non-Cryst. Solids **163**, 74–80 (1993)

Karlsson, G., Pasiskevicius, V., Laurell, F., Tellefsen, J.A., Denker, B., Galagan, B.I., Osiko, V.V., Sverchkov, S.: Diode-pumped Er–Yb:glass laser passively Q switched by use of Co^{2+}:$MgAl_2O_4$ as a saturable absorber. Appl. Opt. **39**, 6188–6192 (2000)

Karlsson, G., Laurell, F., Tellefsen, J., Denker, B., Galagan, B., Osiko, V., Sverchkov, S.: Development and characterization of Yb–Er laser glass for high average power laser diode pumping. Appl. Phys. B **75**, 41–46 (2002)

Kisel, V.E., Gorbachenya, K.N., Yasukevich, A.S., Ivashko, A.M., Kuleshov, N.V., Maltsev, V.V., Leonyuk, N.I.: Passively Q-switched microchip Er, Yb:$YAl_3(BO_3)_4$ diode-pumped laser. Opt. Lett. **37**, 2745–2747 (2012)

Laporta, P., De Silvestri, S., Magni, V., Svelto, O.: Diode-pumped cw bulk Er:Yb:glass laser. Opt. Lett. **16**, 1952–1954 (1991)

Li, C., Moncorge, R., Sourieau, J.C., Borel, C., Wyon, C.: Room temperature CW laser action of Y_2SiO_5:Yb^{3+}, Er^{3+} at 1.57 μm. Opt. Commun. **107**, 61–64 (1994)

Mlynczak, J., Kopczynski, K., Mierczyk, Z., Zygmunt, M., Natkanski, S., Muzal, M., Wojtanowski, J., Kirwil, P., Jakubaszek, M., Knysak, P., Piotrowski, W., Zarzycka, A., Gawlikowski, A.: Practical application of pulsed "eye-safe" microchip laser to laser rangefinders. Opto-Electron. Rev. **21**, 332–337 (2013)

Mlynczak, J., Kopczynski, K., Mierczyk, Z., Malinowska, M., Osiwianski, P.: Comparison of cw laser generation in Er^{3+}, Yb^{3+}:glass microchip lasers with different types of glasses. Opto-Electron. Rev. **19**, 491–495 (2011)

Mlynczak, J., Kopczynski, K., Mierczyk, Z., Malinowska, M., Osiwianski, P.: Pulse generation at 1.5 μm wavelength in new EAT14 glasses doped with Er^{3+} and Yb^{3+} ions. Opto-Electron. Rev. **20**, 87–90 (2012)

Mlynczak, J., Belghachem, N.: High peak power generation in thermally bonded Er^{3+}, Yb^{3+}:glass/Co^{2+}:MgAl2O4 microchip laser for telemetry application. Laser Phys. Lett. **12**, 45803–45807 (2015a)

Mlynczak, J., Belghachem, N.: Monolithic thermally bonded Er^{3+}, Yb^{3+}:glass/Co^{2+}:MgAl2O4 microchip lasers. Opt. Commun. **356**, 166–169 (2015b)

Mlynczak, J., Belghachem, N.: Laser generation in newly developed PAL77 and PAL80 glasses doped with Er^{3+} and Yb^{3+} ions. Laser Phys. **25**, 1–5 (2015c)

Schweizer, T., Jensen, T., Heumann, E., Huber, G.: Spectroscopic properties and diode pumped 1.6 μm laser performance in Yb-codoped Er:$Y_3Al_5O_{12}$ and Er:Y_2SiO_5. Opt. Commun. **118**, 557–561 (1995)

Sourian, J.C., Romero, P., Borel, C., Wyon, C., Li, C., Moncorge, R.: Room-temperature diode-pumped continuous-wave $SrY_4(SiO_4)_3O$:Yb^{3+}, Er^{3+} crystal laser at 1554 nm. Appl. Phys. Lett. **64**, 1189–1191 (1994)

Sulc, J., Jelinkova, H., Ryba-Romanowski, W., Lukasiewicz, T.: 1.6 μm microchip laser. Laser Phys. Lett. **6**, 207–211 (2009)

Zayhowski, J.J., Wilson, A.L.: Miniature eye-safe laser system for high-resolution three-dimensional lidar. Appl. Opt. **46**, 5951–5956 (2007)